APPLICATIONS OF REMOTE SENSING IN LITHOLOGICAL MAPPING OF EAST ESH EL MALAHA AREA, SOUTHWEST GULF OF SUEZ - EGYPT

Adel M. Seleim[1], Mohamed S. Hammed[2]
[1] Geology Department, Faculty of Science Al-Azhar University, Nasr City, 11884, Egypt.
[2] Geology Department, Faculty of Science, Cairo University, Giza City, 12613, Egypt.

Abstract: The East Esh El Malaha area at the southwestern margin of the Gulf of Suez comprises a variety of Precambrian basement rocks of Gebel El Zeit and Esh El Malaha rotated rift blocks, (including Metavolcanics, Older Granites, Dokhan volcanics, Hammamat sediments and Younger Granites) in addition to the sedimentary cover of Paleozoic-Quaternary sediments at their hogbacks. Lithological mapping and rock unit discriminations of the East Esh El Malaha area were carried out by using the image processing techniques of the color composite image and spectral signature analysis (SSA) of Landsat-8 (OLI) remotely sensed data. The principal component analysis (PCA) besides the band ratios of (4/5, 5/7, 3/1 RGB), (7/3, 7/6, 2/5 RGB) and (3/4, 4/6, 2/1 RGB) were efficiently applied with improvement over the previous techniques in lithological discrimination of the main rock units. Additionally, it was able to discriminate the granitoid of the main Gebel El Zeit into two phases of the Older Granites and three phases of the Younger Granites. The supervised classification technique fruitfully helps in tracing the contacts of thirteen mappable lithological units of the Precambrian basement and Phanerozoic sediment rocks.
The aforementioned techniques with field verifications help to improve lithological identification and distribution of the main rock units and construct a new digital version of the lithological map of East Esh El Malaha area.

Index Terms: LANDSAT-8, BAND RATIO, SUPERVISED CLASSIFICATION, EAST ESH EL MALAHA EGYPT.

1-INTRODUCTION

EAST Esh El Malaha area lies at the southwestern margin of the Gulf of Suez rift between latitude 27º 19 11 to 28º 00 06 N and longitude 33 º 18 30 to 33 º 39 53 E. The economic importance of the area is reflected by the presence of than 15 offshore and onshore oil fields. The study area comprises two basements cored rotated rift blocks, namely Gebel El Zeit and Esh El Malaha, overlain by a stratigraphic sequence of Paleozoic-Quaternary sediments at their hogbacks. Detailed mappings of these exposed rift blocks are the core stone in subsurface analog studies in oil exploration and characterization of the Precambrian basement reservoirs [1], [2]. During the last two decades, remote sensing data have been efficiently applied to map and interpret different surface and near-surface parameters e.g., mineralogical, chemical and physical characteristics of geological formations [3], [4]. Lithological mapping by a Landsat band ratio has been used by several authors [5], [6], and [7]. The present work utilizes the image processing techniques on the Landsat-8 Operational Land Imager (OLI) data in lithological discrimination of the various exposed rock units at the East Esh El Malaha area with field verification.

2- GEOLOGIC SETTING

The Gulf of Suez rift is the northwestern extension of the Late Tertiary Red Sea rift system [8], [9]. It is a prolific extension basin with three asymmetric dip provinces and maximum stretching in the southern one including the study area [10]. Outcrops in the East Esh El Malaha area, range from Precambrian crystalline basement rocks to recent sediments (Fig.2) [11], [2].
The structure of the southwestern margin of the Gulf of Suez is dominated by three main extensional fault systems, the Rift Border Fault, East Esh El Malaha Rift fault system and the Rift Coastal fault system of East G. El Zeit [12]. The last two faults are in the study area and all of these are hard linked normal fault segments in zigzag arrays and of two dominant strikes Gulf parallel NW-trending and Gulf orthogonal ENE-trending faults [13]. The plain area between the two basement blocks is a sedimentary depocentre known as west G. El Zeit (Gemsa) basin (Fig.1).
The Pan-African basement of granitoid, volcanics, sediments, and dikes are exposed in the Gebel E Zeit and Esh- El Malha fault blocks (Fig.2). These rocks are grouped in four Late Precambrian rock units, namely, 1) Metavolcanics 2) Older granites 2) Dokhan volcanics, 3) Hammamat sediments 4) Younger granites [14]. The basement of Gebel El Zeit forms two sub-blocks, the Main Zeit and Little Zeit separated by sediments of Sarg El Zeit. Both of them have multiple intrusions of granodioritic to granitic rocks are known as the Older Granite (gray) and younger Granite (pink) and Dokhan volcanicss which were emplaced during the Precambrian cratonization of the Arabo-Nubian shield [8]. A southwest-dipping sedimentary sequence of Gebel El Zeit aligned along Wadi Kabrite as Sufr Gebel El Zeit Range. This sequence comprises a thick pre-rift section of Paleozoic-lower Cretaceous clastics of Nubia sandstones and upper Cretaceous-Eocene mixed clastics and carbonates unconformably overlies the Precambrian basement [15]. The upper Cretaceous sequence includes sandstones and shales of Cenomanian Raha Formation, limestone of Turonian Wata Formation, thick sandstones and shales of Coniacian-Santonian Matulla Formation and Campanian-Maastrichtian Sudr Chalk [16], [17]. The Eocene rocks have a limited occurrence at the apex of Sufr Gebel El Zeit.
Syn- to post-rift strata range from Miocene to Quaternary age and rest with a major angular unconformity over the pre-rift rocks [18], [19]. The Miocene rocks include distal and proximal facies of shallow-marine calcareous sandstones and conglomerates, open-marine marls, reefal carbonates and interbedded evaporites and shales. They are classified here as Nukhul/Abu Gerfan, Rudies-

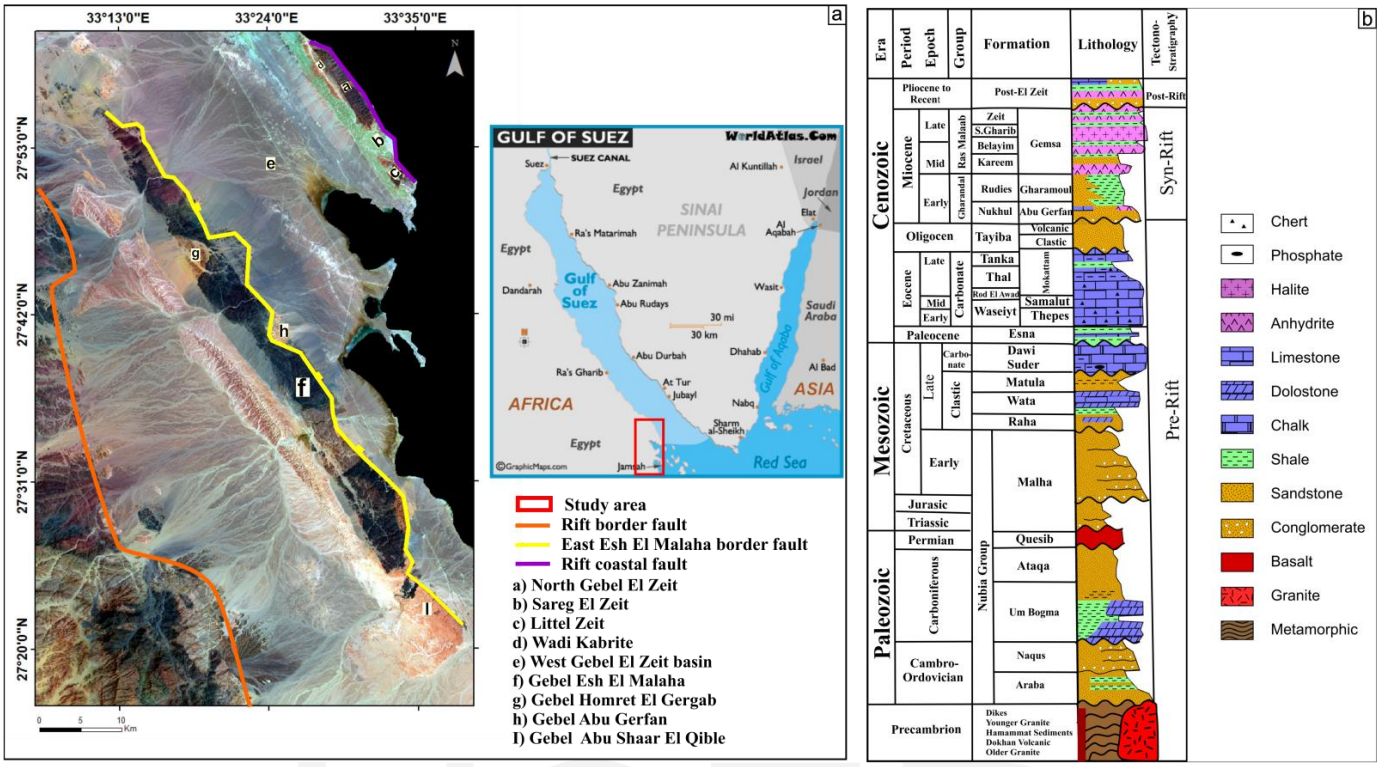

Fig.1: a) Location map (right) and Landsat 8 RGB 742 image shows the physiography and main structures of the study area (left)
b) Generalized stratigraphic column of the study area (Modified after Darwish and El Azabi., 1993)[20]

Kareem/Gharamoul, Belayim-South Ghareib-Zeit/Gemsa formations [20], [10], [2]. The Pliocene to Quaternary deposits includes alluvial fans, beach deposits, coastal fan deltas and wind-blown sands on the wadi floors. The Early Miocene sediments of Abu Gerfan/Nukhul Formation occur in a sedimentary nitch of Abu Gerfan outcrop within the central Esh El Mallaha basement block as thin reddish brown conglomerate and sandstone. The sandstone with thin shale beds are overlain by a dominant carbonate platform of Gharamoul Formation at Abu Shaar El Qabli and Sufr El Zeit. The evaporates and carbonate of Gemsa Formation and Pliocene sediments occur at the down-dip of Sufr El Zeit and around Gemsa Bay [20].

3- DATA SETS AND METHODS

3.1 Landsat-8 data

The remotely sensed data used in this study originates from Landsat-8, which has been launched in February 2013 and is currently operated by the EROS Data Center of the United States Geological Survey. Newly Landsat 8 operational land Imager (OLI) has a wide used and provide the capability in the lithological discrimination of different rock units [6], [7], [21]. It comprises nine spectral bands with a spatial resolution of 30 meters for Bands 1 to 7 and 9. New band 1 (ultra-blue) is useful for coastal and aerosol studies. New
band 9 is useful for cirrus cloud detection. The resolution for Band 8 (Panchromatic) is 15 meter. The OLI scene of path 174/041 row, UTM projection of zone 36 and WGS-84 datum, which is here, have been acquired in August 2014.

3.2 PRE-PROCESSING

The pre-processing and processing of the OLI scene data covering the area was performed by using the ENVI 5.1, ARC GIS 10.1 and ILWES 3.4 software. The pre-processing steps include atmospheric correction, removing the unwanted noise; correction for instrumental and geometric errors, re-scaling the raw radiance data from imaging spectrometer to reflectance data and finally masked the water band. The data was also calibrated to spectral radiance, subset, and convert from the digital number (DN) to reflectance by FLAASH algorithm.

3.3 IMAGE PROCESSING TECHNIQUES

Different image enhancement and processing techniques were executed on the corrected reflectance Landsat-8 data aim at lithological mapping and discrimination of the exposed rock units the study area, as following:

1- By applying the optimum index factor (OIF), the best the RGB band composite images were selected based on standard deviation and correlation coefficients [22].
2- The principal component analysis (PCA) reduces the data redundancy and yields more contrasting bands.
3- Spectral signature analysis was applied to identify each lithological units and the discrimination of the exposed rock units in the study area improved by the band ratios transformation images.
4- Supervised classification technique with the aids of field verification was used to construct a new lithological map showing the different rock units.

3.3.1 Band combination using OIF

The Landsat-8 data contains the widest possible range of multispectral data in RGB band combination. Seven bands Landsat-8

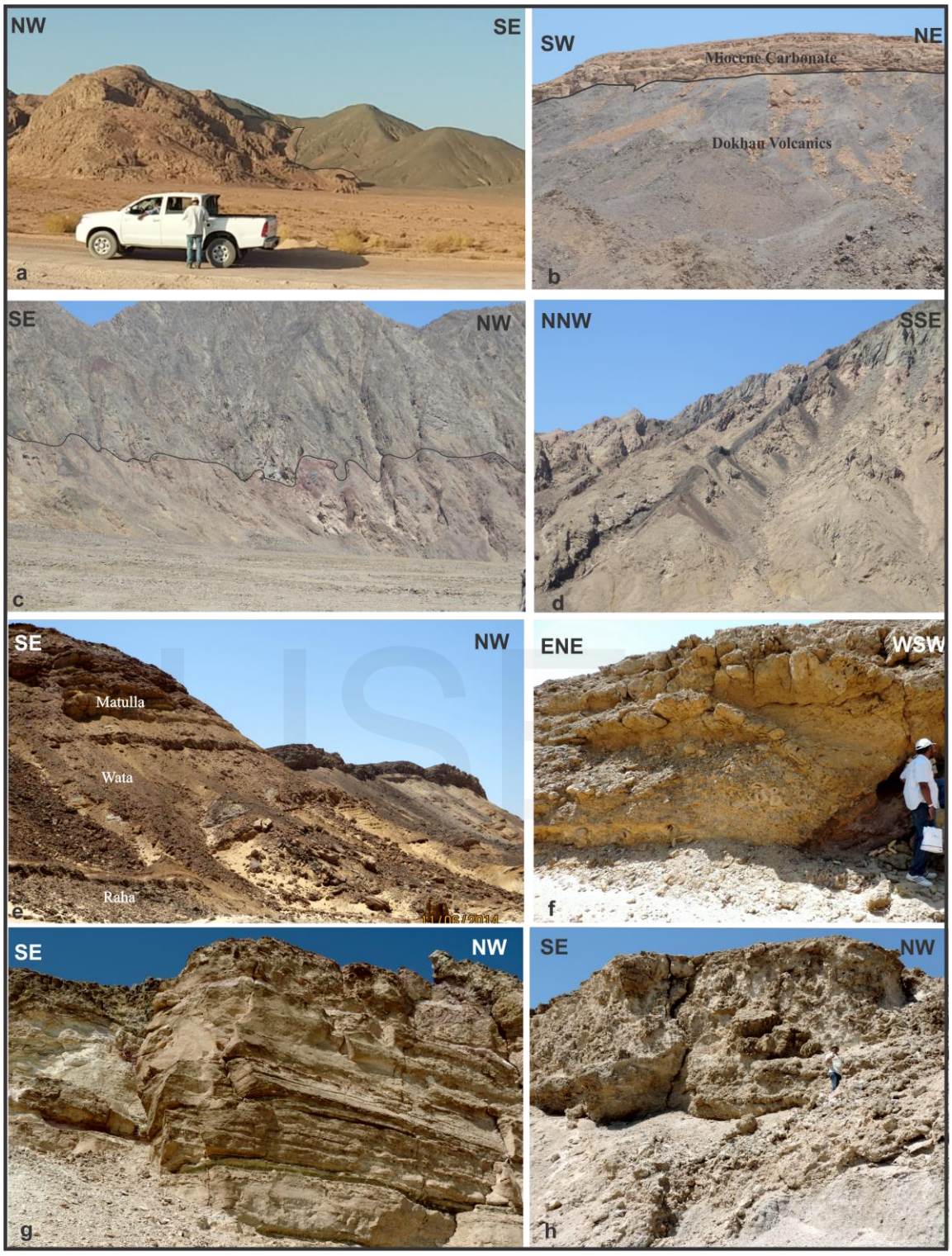

Fig.2: Field occurrences of the exposed rock units in the study area:
a)Younger Granite intruded in Dokhan volcanics at Gebel Homret El Gergab, b)Dokhan volcanics capped with Miocene carbonate, Wadi Bali.,
c) Two phase of Younger Granites (monzogranite and syenogranite), Eastern side of Main Zeit, d) Basic dike cut the older granite, Wadi Kabrite.
e) Upper Cretaceous sequence of Raha, Wata and Matulla formations at, Wadi Kabrite, f) Dokhan volcanics/Miocene carbonate at AbuShaar El Qabli,
g) Carbonate intercalated with shale and marl of Gemsa Fm (Belayim Fm) at Ras Gemsa, and h)Pleistocene reefs as raised beaches, Little Zeit.

are imported into the ELWIS 3.4 software to calculate and select the most informative color composite images for the present study. The best band combination of the highest sum of standard deviations and lowest correlation among band pairs is selected. Considering the correlation matrix, the (7, 4, 2 RGB) image shows the highest OIF of all combinations, it should give the best lithological discriminating, due to the high content of variance (90.61%).

3.3.2 Principal Components Analysis (PCA)

The PCA is used for lithological feature detection from Landsat-8 (OLI) data. The seven PCs bands were deduced from the Landsat-8 data includes visible-NIR and SWIR. Analysis of PCs eigenvector loading gave a clear idea about the selection of the bands, which enhance the color differences between the rock types (Fig.3.a). The eigenvalues show high positive loading, high negative loading and near zero loading indicate a positive correlation, negative correlation, and the lack of correlation of the original bands data, respectively (Fig.3.b). The first three PCAs contained approximately 99.8 % of information where the PC1 contain 98.6%, the PC2 contain 1.03% and the PC3 contain 0.19 %. The last PCA bands appear noisy as they contain a little variance data, however, they keep the ability to discriminate the lithological rock units in the field region [23]. The visual investigations of the seven PCA bands in grayscale (Fig.3.a) revealed the followings; 1) The PC1 highlights basement and sedimentary rocks especially early Miocene where it is appearing with bright color, 2) The PC2 distinguishes the Dokhan volcanics with brightness color from the Alkali feldspar granite as well as Lower Cretaceous and Lower Miocene with dark color, 3) The PC3 and PC4 distinguish between Metavolcanics and Dokhan volcanics at the northern part of Esh El Malaha, 4) The PC5 distinguishes well between Phanerozoic sedimentary rock units of Paleozoic-Lower Cretaceous (Nubia sandstones), Lower and Middle Miocene, 5) PC6 can discriminate between the three different types of granitoid at Gebel El Zeit and 6) The PC7 is a noisy band, it may be representing the zone that masked due to a high absorption value of water and so it is excluded from the classification.

Based on the above result of the PCA, the best RGB composite images of maximum lithological discrimination turned out to be (PC2, PC1, PC3), (PC5, PC3, PC2) and (PC4, PC5, PC2) RGB images (Fig.4).

3.3.3 Band ratio

The band ratio technique is the ratio of one band to another. It was applied simply by dividing the DN of each pixel in one band by the DN of another band [24]. Different band ratio composite images were prepared from Landsat-8 (OLI) data. The tested band ratios suggested from previous studies (Fig.5) [5], [7]. The band ratio (5/7, 4/5, 3/1 RGB) Landsat TM image was created to map the units of Neoproterozoic Allaqi Suture at the Southeastern Desert of Egypt [5]. Recently, the band ratio (6/2, 6/7, 6/5 X 4/5 RGB) of Landsat-8 data was used to discriminate between the acidic, basic and intermediate metavolcanics as well as Hammamat sediments at Abu Marawat area, Eastern Desert, Egypt [7].

Analysis and comparing the results of spectral signature profiles of the exposed rock units (Fig3.c) indicate the following:

a. The examined spectral curves, which extracted from the band combination (7, 4, 2 RGB) image show a characteristic reflectance value with band 6 (SWIR), high absorption feature of visible band 2 and low absorption of band 3 and 4, and band 5. This means the true color composites will not be useful to discriminate the various lithologyof the study area. Thus, the false color composites of these band combinations and ratios will facilitate and enhance discriminations between the different rock units.

b. The spectral profiles of the Precambrian and Phanerozoic rocks show the general reflectance differences for all bands Hence, the different ratios of these bands will be a significant discrimination tool.

c. Most of the present lithologies are characterized by different absorption features for various bands. These designate the value of band ratio such as 2/1, 4/5, 3/1, 7/6, 2/6, 5/6, 4/3, 4/6, 5/7.

d. Based on the spectral reflectance profiles (Fig.3.c), the following proposed band ratio (4/5, 5/7, 3/1 RGB), (7/6, 5/6, 2/6 RGB) and (3/4, 4/6, 2/1 RGB) were powerfully tested (Fig.5).

3.3.4. Mahalanobis Distance:

A direction-sensitive distance classifier that uses statistics for each class assumes all class covariances are equal, and therefore is a faster method. All pixels are classified to the closest interest data of the ENVI implements Mahalanobis Distance classification. This is carried out by calculating the following discriminate functions for each pixel in the image [25].

$$D_i(x) = \sqrt{(x - m_i)^T \sum_i^{-1} (x - m_i)}$$

Where:

D = Mahalanobis distance

i = the class

x = n-dimensional data (where n is the number of bands)

Σi-1 = the inverse of the covariance matrix of a class

mi = mean vector of a class

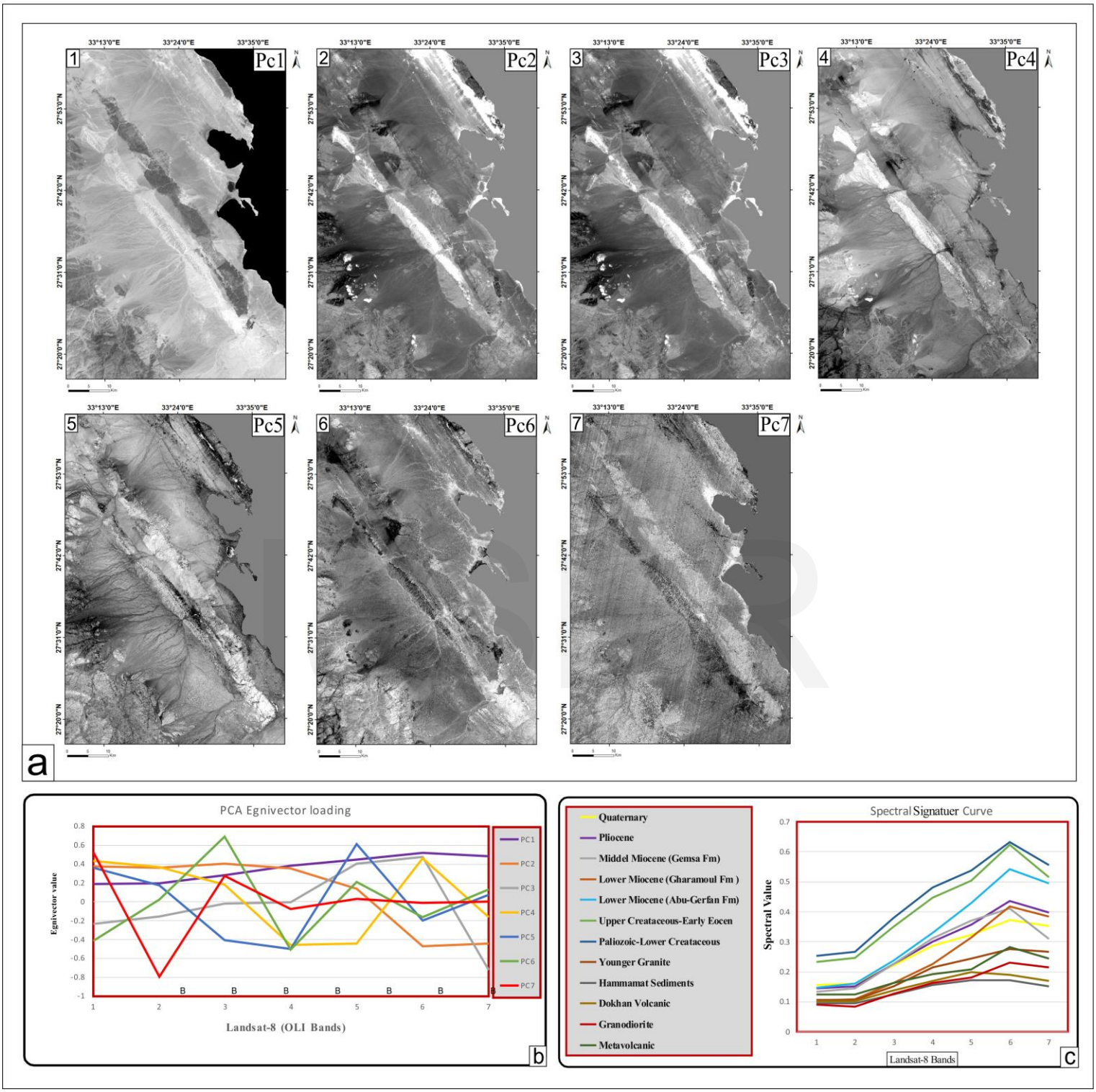

Fig. 3: a) The seven Pcs generated from the Landsat-8 visible, NIR, SWIR bands covering the study area, b) PCA loading show the correlation in the original bands, and c) Spectral signature analysis for the exposed rock units

4 - RESULT

This present study utilized different remote sensing image processing techniques as OIF, color composite image, spectral analyst, band ratio and supervised classification. The selection of band combina tions depends on statically method (OIF) to select the most informative color composite image. Band composite images (7, 4, 2 in RGB)

are more varied and suitable for the rock units of the study area and provide an excellent base map in which rock units are easily discriminated (Fig.1.a).

The best PCA transformation was selected according to corresponding eigenvector loadings and the applicability for enhancing different rock types turned out to be

The (PC2, PC1, PC3) RGB image shows high contrast between basements rocks at North Esh El Malaha, where we can discriminate between the Metavolcanics, Dokhan volcanics, Monzogranite and Alkali-Feldspar granite (Fig.4.a).

The (PC4, PC5, PC2) RGB image has better contrast between the two types of younger granitoid (Monzogranite and Alkali Feldspar Granite), Paleozoic-Lower Cretaceous, Upper Cretaceous, Abu Gerfan formation, Gharamoul formation and Gemsa formation at North Gebel El Zeit (Fig.4.b).

The (PC5, PC3, PC2) RGB gave better discrimination between Nubia sandstone, Abu Gerfan and Gemsa formation at Gebel Abu Gerfan (Fig.4.c).

Different band ratios were as prepared by tested previous band ratio and ratio, which gave high contrast and have the ability to discriminate the different lithological rock units characterized the study area.

Band ratios (4/7, 3/4, 2/1) of ASTER image [5] which are equivalent to (5/7, 4/5, 3/1) Landsat-8 (Fig.5.a), discriminate the Precambrian and overlay Paleozoic-Quaternary rocks into four categories with low sharp contact between different lithological units where the Mata-volcanics appear with green as well as the younger Granit and Quaternary sediments, the Dokhan volcanics appear with yellow color, Lower Miocene appear with blue color and the Middle Miocene appear with pink color.

Band ratio (7/6, 6/5, 6/4 RGB) as used for mapping gneiss domes and granites in south Tibet [6], gave bad result where it was giving low contrast between different rock units (Fig.5.b)

Band-ratio image (6/2, 6/7, 6/5 x 4/5) of Landsat-8 data used to discriminate acidic, basic and intermediate Metavolcanics as well as Hammamat sediments [7]. The band ratio distinguishes the Precambrian rocks into two categories where the basic rocks (Dokhan volcanics) appear with green color while the other lithological rocks appear with violet color (Fig.5.c)

The first new proposed band ratio (7/6, 5/6, 2/6 RGB) (Fig.5.d)

discriminates the Precambrian rocks into five categories where the Metavolcanics appear with orange color, the Dokhan volcanics appear with light color, younger granite with red color, Lower Miocene appear with deep red while the Middle Miocene appear with blue color.

The second new proposed band ratio (4/5, 5/7, 3/1) (Fig.5.e) discriminate the exposed rocks into the Metavolcanics, Dokhan volcanics, Esh El Malaha and of Gebel El Zeit younger Granite, Lower Miocene and Middle Miocene as red, yellow, violet, pale red, blue, and sky blue colors, respectively.

Classification of G. El Zeit Granitoids(Fig.4)

The third new proposed band ratio (3/4, 4/6, 2/1 RGB) has the ability to discriminate the main basement rock units. The Main Gebel El Zeit was considered as one type of alkali younger granite on the old maps (Conco, 1987). The new band ratio differentiates the Gebel El Zeit granite into five granitoid types. Those are classified here as two phases of Older Granite and four phases of Younger Granite, which are assigned as G1, G2, G3, G4, G5 and G6 respectively (Fig.5.f).

Mahalanobis Distance classification for the rock units of the area (Fig.6)

Mahalanobis Distance classification gave the best result with the high accuracy (95%), where it distinguished 13 classes, to 13 colors corresponding to a certain rock unit (Fig.6). By using the classification result, combined with field verifications, a new geological map could be created. The new lithological map (Fig.7) shows more clear improvement and variations than a previously published map. It gave high resolution and a better exclusion for rock units especially basement rocks. Many lithological units have a new set of the border and the others were sustained. Also, some rock units are reclassified as a different unit than before, e.g. discriminate the granitoid of the North Gebel El Zeit into two phases of the Older Granites and four phases of the Younger Granites.

5-CONCLUSION

The purpose of this study was to hold an investigation using Landsat-8 data to map the lithological units in East Esh El Malaha area. Various image processing techniques applied to produce derivative data sets that contained enhanced information according to lithological discrimination. These enhancement techniques combined with the field observation and previous lithological mapping studied in the East Esh El Malaha, allow distinguishing between the different rock units. There are band ratios were used by several authors, to develop the best tool in geological mapping of the arid region [5], [6]. In general, these ratios concerned with basement rock mapping in the Eastern Desert and/or tried to distinguish one kind of rock units [5], [6] and [7]. The present work used the same techniques in addition to Principal component analysis to discriminate between basement rocks (high absorption) and the sedimentary rocks (high reflectance). The spectral signature analysis was helpful to select the best bands in the ratio technique. The new proposed band ratios provide better result than the previously published ones. They are not only discriminate between the basement and sedimentary rocks but also it distinguishes between the basement itself (Metavolcanics, Granodiorite, Dokhan volcanics, Hammamat sediments, Monzogranite, and Alkali feldspar granite) and Sedimentary rocks (Nubia sandstones, Abu Gerfan formation, Gharamoul formation, Gemsa Formation and Quaternary). It was also powerful tool to classify the five granitic rocks of G. El Zeit. The Mahalanobis Distance classification gave the most significant result among the other supervised classification algorisms where it has high accuracy assented (95%). Finally, these techniques are integrated to construct a new lithological map of East Esh El Malaha area with after field verification.

6 – ACKNOWLEDGEMENTS

The present authors thank Dr. M. Bekhait at the geology department, Azhr University for his constructive assistance during the fieldwork of the first author and improving the manuscript.

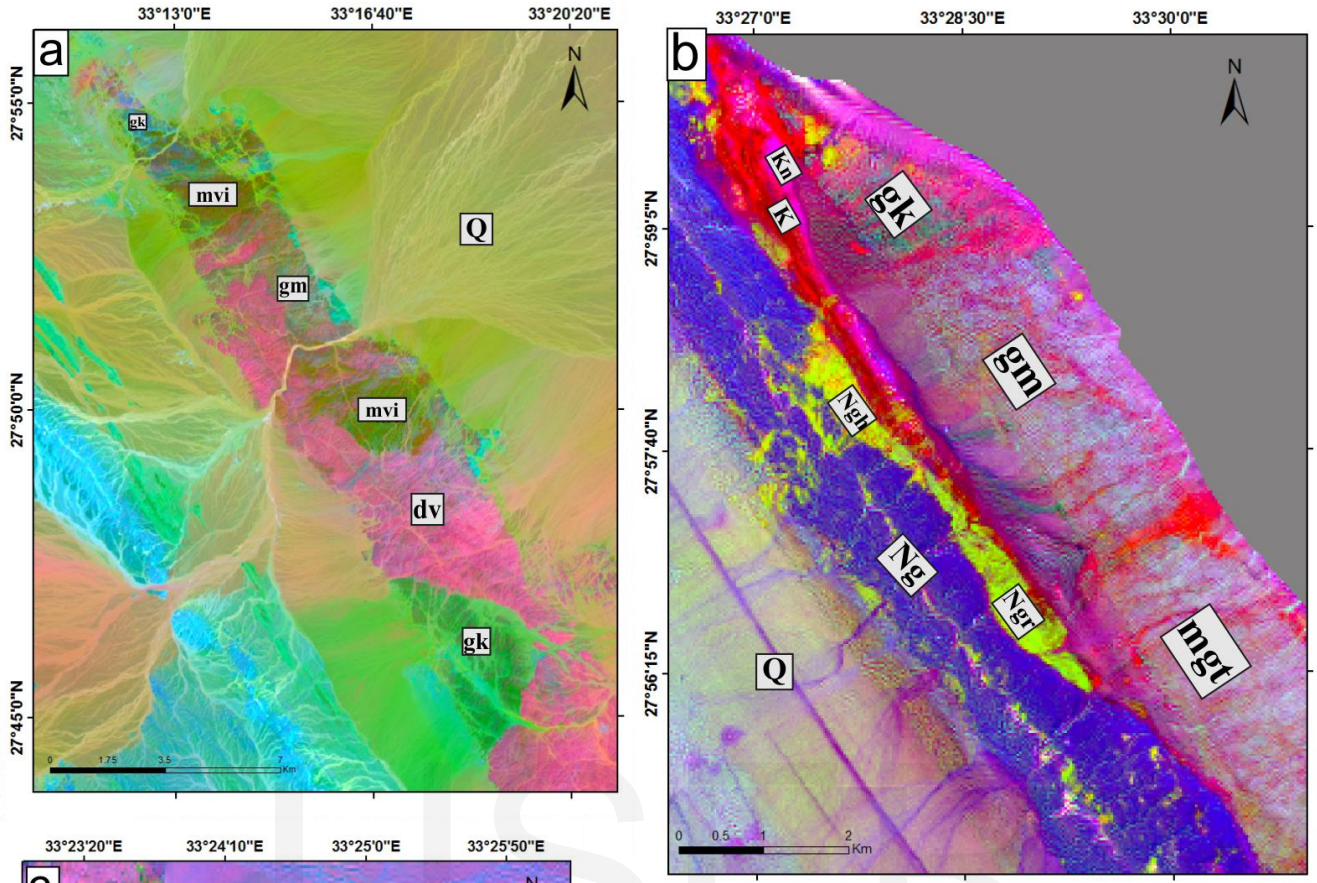

Fig.4: Results of the Principle Component Analysis (PCA) at selected localities of the Study area:
a-(PC2, PC1, PC3 RGB) North Esh El Malaha range
b-(PC4, PC5, PC2 RGB) North Gebel El Zeit
c-(PC5, PC3, PC2 RGB) Abu Gerfan

Precambrian basement rock units
mvi: Metavolcanics, **dv:** Dokhan volcanics,
mgt: granodiorite, gm: Monzogranite,
gk: Alkali-feldspar granite.
Phanerozoic sedimentary rock units
Kn: Paleozoic- Lower Cretaceous (Nubia group),
k: Upper Cretaceous,
Ngr: Lower Miocene Abu Gerfan Formation,
Ngh: Gharamoul Formation, **Ng:** Gemsa Formation,
Q: Quaternary

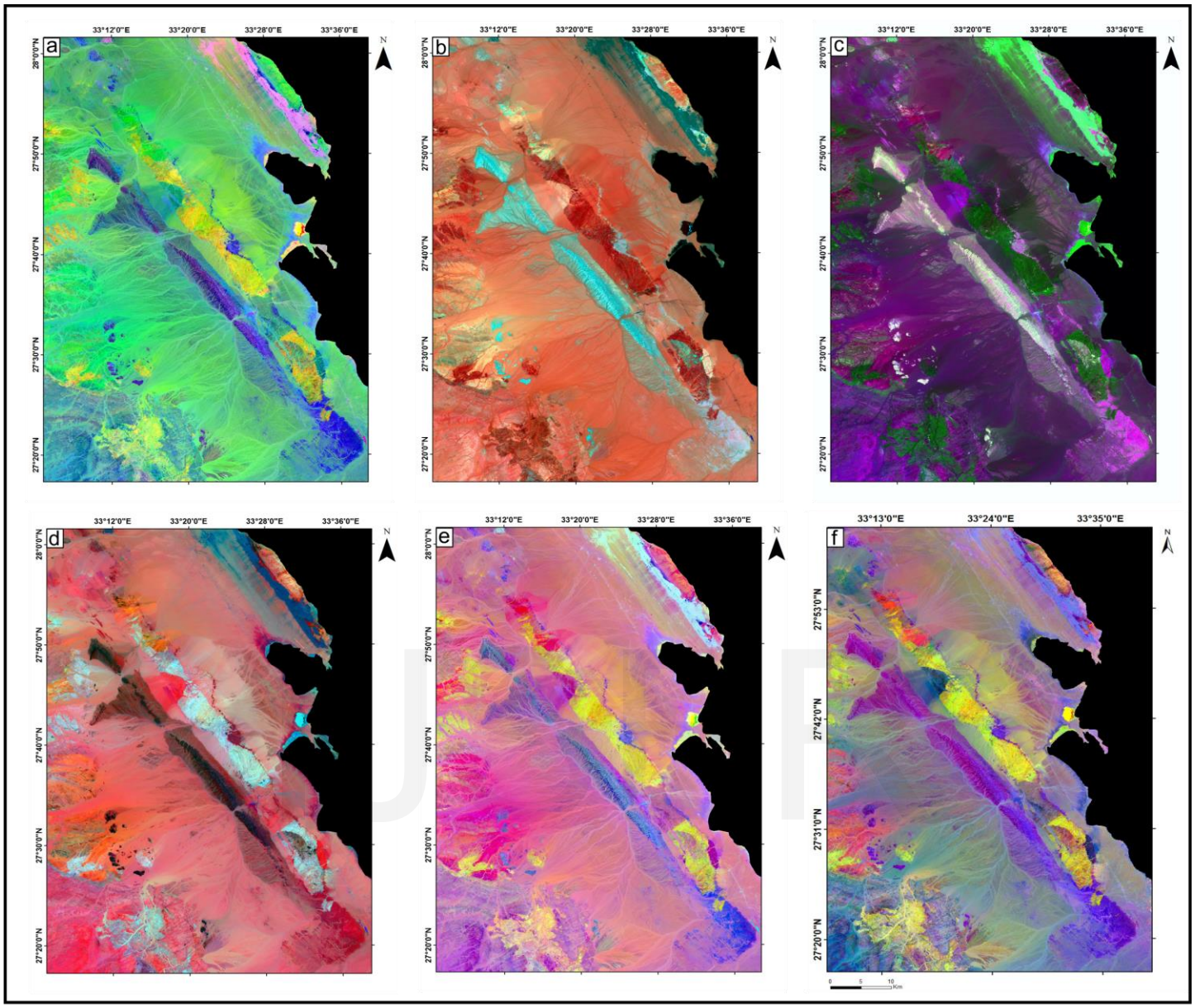

Fig.5. Comparison between band ratios in previous studies and the proposed by the present work.

a) 5/7, 4/5, 3/1 RGB [5]
b) 7/6, 6/5, 6/4 RGB [6]
c) 6/2, 6/7, 6/5*4/5 RGB [7]
d) 7/6, 2/6, 5/6 RGB
e) 4/5, 5/7, 3/1 RGB
f) 3/4, 4/6, 2/1 RGB

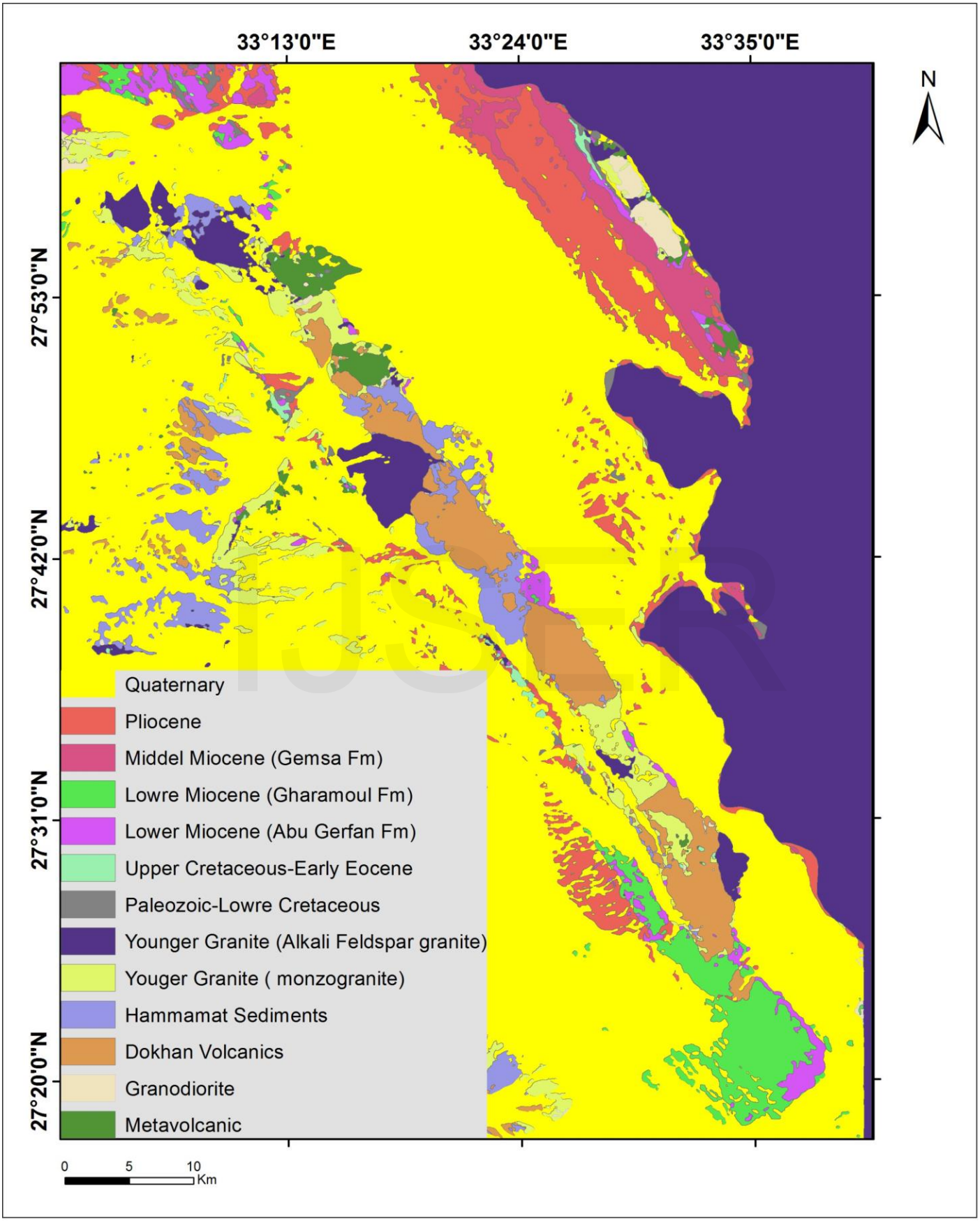

Fig. 6. The Mahalanobis Distance classification map of the study area.

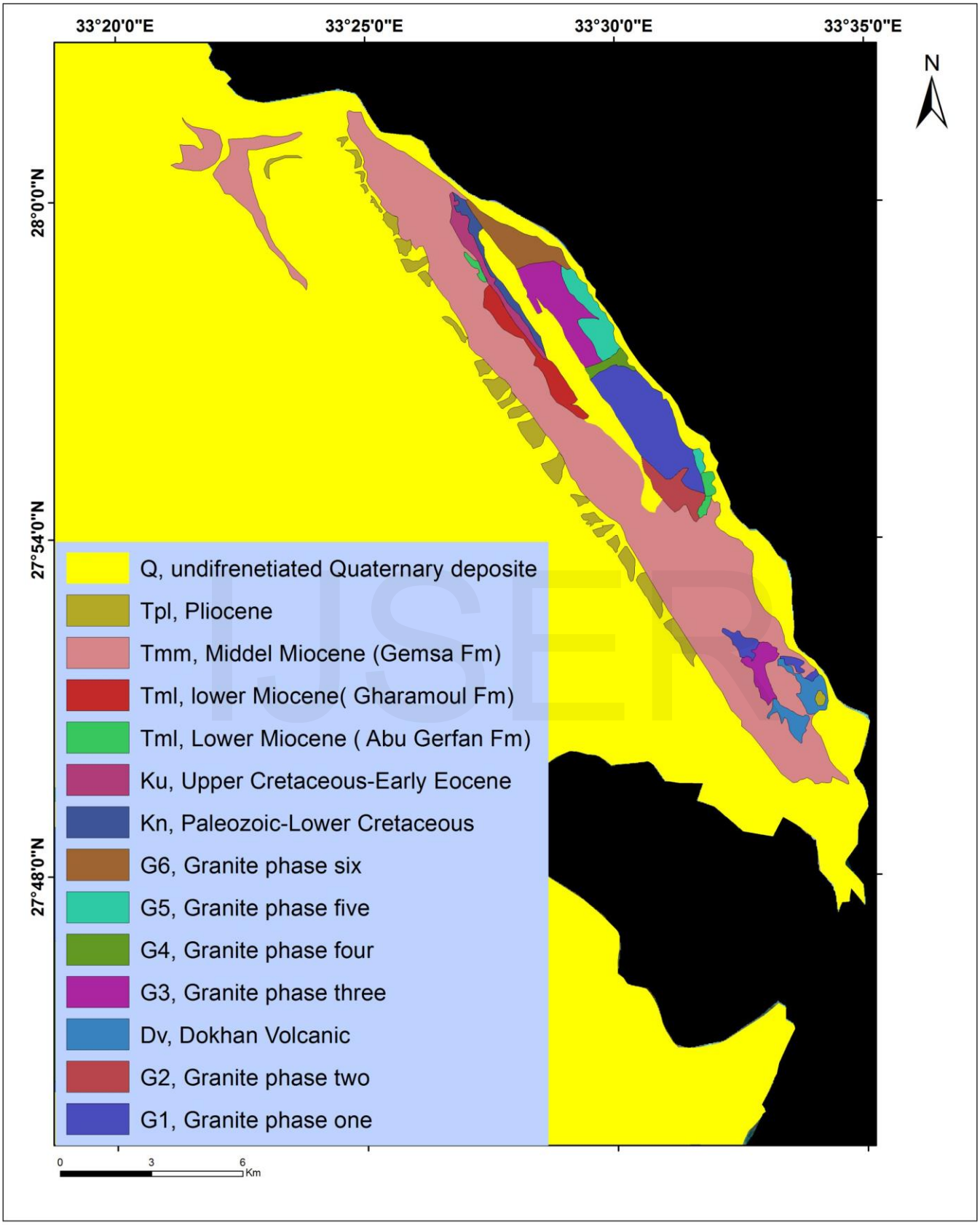

Fig.7.Geological map Of Gebel El Zeit

7 - REFERENCES

[1] Younes, A and McClay, K. 1998. The role of basement fabric on Miocene rifting in the Gulf of Suez-Red sea proceedings of the 14th EGPC Exploration., Vol.1. Production conference, Cairo, pp.35-50.

[2] Hammed, M.S. 2002. Geology and structural architecture of southwest Gulf of Suez, with special emphasis on the Precambrian rocks of gebel el zeit area, Egypt. Ph.D. Thesis, Cairo Univ., Egypt.

[3] Rowan, L. C. and Mars, J. C., 2001. Advances in lithologic mapping by using optical remote sensing measurements, Geological society of America, 33, 347 p.

[4] Cudahy, T. H. and Hewson, R., 2002. ASTER geological case histories: Porphyry-skarnepithermal, iron oxide, Cu-Au and Broken Hill Pb-Zn-Ag. Communication in the Workshop Mapping the Earth with ASTER, London.

[5] Abdeen, M.M., Allison, T.K., Abdelsalam, M.G., und Stern, R.J., 2001. Application of ASTER band-ratio images for geological mapping in arid regions; the Neoproterozoic Allaqi Suture, Egypt. Abstr. Program Geol. Soc. Am. 3, 289.

[6] Wolters, J.M., Goldin, L., Watts, D.R., Harris, N.B.W., 2005. Remote sensing of gneiss and granite in southern Tibet. Geol. Soci. Am. Abstr. Program 37 (5), 93.

[7] Hassan, S.M., Ramadan, T.M., 2015. Mapping of the late Neoproterozoic basement rocks and detection of the gold –bearing alteration zones at Abu Marawat-Semna area, Eastern desert, Egypt using remote sensing data. Arabian J. Geoscience 8, 4641-4656.

[8] Patton, T.L., Moustafa, A.R., Nelson, R.A., Abdine, S.A. 1994. Tectonic evolution and structural setting of the Suez rift. In: Landon, S.M. (ed.) Interior Rift Basins. American Association of Petroleum Geologists Memoir 59: pp. 9–55.

[9] Bosworth, W., McClay, K.R., 2001. Structural and stratigraphic evolution of the Gulf of Suez Rift, Egypt, a synthesis. In: Ziegler, P.A., Cavazza, W., Robertson, A.H.F., Crasquin-Soleau, S. (eds.), Peri-Tethys Memoir 6: Peri-Tethyan Rift/Wrench Basins and Passive Margins, vol. 186. Memoirs du Musée National D'Histoire Naturelle, pp. 567–606.

[10] Bosworth, W. 1995. A high-strain rift model for the southern Gulf of Suez (Egypt). In: Lambiase, J. J. (ed.). Hydrocarbon Habitat in Rift Basins. Geological Society, London, Special Publications. v. 80. p. 75-102.

[11] Bosworth, W., Crevello, P., Winn JR., R.D. & Steinmetz, J., 1998. Structure, sedimentation, and basin dynamics during rifting of the Gulf of Suez and northwestern Red Sea. In: B.H. Purser & D. W.I. Bosence (eds.), sedimentation, and Tectonics of Rift Basins: Red Sea Gulf of Aden. Chapman and Hall, London: 77-96.

[12] Hammed M. and Sehim, A. 2002. Rift border fault system evolution and its impact on sedimentation, Southwestern Gulf of Suez, Egypt, Abstracts of AAPG, International Convention – Cairo, Egypt.

[13] Morley, C.K., 1995. Developments in the structural geology of rifts over the last decade and their impact on hydrocarbon exploration. In: Lambiase, J., (ed.), Hydrocarbon habitat of rift basins, Geological Society of London, Special Publication, 80., pp. 1–32.

[14] Abdel Rahman, A.M. and Martin, R.F. 1987. Late Pan-African magmatism and crustal development in northeastern Egypt. J. Geol., 22, 281-301.

[15] Abdallah, A.M. and Adindani, A. 1963. Stratigraphy of Upper Paleozoic rocks, western side of Gulf of Suez. Geol. Surv. Egypt, Paper No. 25, 18p.

[16] Ghorab, M.A. 1961. Abnormal stratigraphic features in Ras Gharib oil field. The 3Arab Petrol. Conger. Alexandria, Egypt, 10p.

[17] Youssef, M.I. 1957. Upper Cretaceous rocks in Kosseir area. Bulletin of Desert Institute Egypt, 7: 35-54.

[18] Abd El Motaal, E. 1993. Structure studies on the sedimentary cover along the coastal area of the Red Sea between Lat. 26 00 and 25 45 N, Egypt. Ph.D. thesis, Geology Dept, Fac. Sci., Azhar Univ., Egypt.

[19] Robert, D., Winn Jr., Crevello, P. D. and Bosworth, W. 2001. Lower Miocene Nukhul formation, Gebel El Ziet, Egypt: A model for structural control on early synrift strata and reservoirs, Gulf of Suez. AAPG Bulletin, v. 85, No.10, pp. 1871-1890.

[20] Darwish, M. and El Azabi, M. 1993. Contributions to the Miocene sequences along the Western Coast of the Gulf of Suez, Egypt. Egyptian Journal of Geology, 37, p. 21-47.

[21] Beiranvand P. and Hashim. M. A. 2014. The application of Landsat-8 OLI/TIRS data for geological mapping: A case study from SE Iran.

[22] Chavez, P. S., Berlin, G. L., Sowers, L. B., 1984. A statistical method for selecting Landsat MSS ratios. J. Appl. Photogr. Eng. 8 (1), 23e30.

[23] Amer, R., Kusky, T., and Ghulam, A., 2010. Lithological mapping in the central eastern desert of Egypt using ASTER data. J. Afr. Earth Sci. 56, 75e82.

[24] Drury, S. A., 1987. Image Interpretation in Geology. 1st. ed., 243 p., (Allen&Unwin) London.

[25] Richards, J. A. 1999. Remote Sensing Digital Image Analysis, Springer-Verlag, Berlin, 240p.

[26] Kruse, F. A., Lefkoff, A. B., Boardman, J. B. Heidebrecht, K. B., Shapiro, A. T., Barloon, P. J. and Goetz, A. F. H. 1993. The Spectral Image Processing System (SIPS) – Interactive Visualization and Analysis of Imaging Spectrometer Data." Remote Sensing of the Environment, 44, p.145 - 163.